PFC/JA-90-12

Observations of Periodic Intensity Bursts from a Free-Electron Laser Oscillator

E. Jerby, G. Bekefi and J. S. Wurtele

April 1990

Department of Physics
Research Laboratory of Electronics
and
Plasma Fusion Center

Massachusetts Institute of Technology
Cambridge, Massachusetts 02139 USA

This work is supported in part by the National Science Foundation, the Air Force Office of Scientific Research and the Naval Research Laboratory. E.J. is supported by the Rothschild and Fulbright foundations.

Submitted for publication in Physical Review Letters.

Observations of Periodic Intensity Bursts from a Free-Electron Laser Oscillator

E. Jerby[†], G. Bekefi and J. S. Wurtele

Department of Physics
Research Laboratory of Electronics
and
Plasma Fusion Center

Massachusetts Institute of Technology
Cambridge, Massachusetts 02139

Abstract

Observations of periodic intensity bursts from a free-electron laser oscillator operating in the microwave regime are reported. Their periodic separation (~40 ns) equals the radiation round-trip time, and their width is approximately the slippage time (~2-4 ns). Unlike previous studies, the bursts occur in the small signal regime, near oscillation threshold. The observations are compared with theoretical results from an impulse response model of the free-electron laser.

[†]Permanent address: Faculty of Engineering, Tel Aviv University, Ramat Aviv, 69978 Israel.

The study of the frequency spectrum and temporal evolution of electromagnetic pulses in lasers is a subject of considerable interest. In conventional atomic and molecular lasers short pulse phenomena have been known for many years. These include the nonlinear phenomenon of self (spontaneous) spiking[1] as well as a wide range of mode-locking mechanisms[2] and soliton formation.[3]

In free-electron laser (FEL) oscillators, radiation bursts, or spikes, as they are often called, have been studied experimentally and theoretically in the nonlinear regime by several groups.[4-10] Their appearance comes about as a result of the FEL side-band instability caused by electron oscillations in the potential wells of the ponderomotive wave. In contrast, studies in this letter[11] deal with the build-up of short electromagnetic pulses well before saturation and near oscillation threshold, where linear phenomena dominate the interaction. The observed spikes have a temporal separation corresponding to the radiation transit time (~40 ns) in the cavity, and their widths (2-4 ns) are believed to correspond to the slippage time between the radiation pulses and the electron bunches. Each assembly of micropulses is contained within a well-defined "macropulse" of about 1μs duration. Although the macropulses occur at random times, their appearance is correlated with observed random current spikes in the electron beam.

Figure 1a shows a schematic of our experiment.[12] The accelerating potential is supplied by a Marx generator (Physics International Pulserad 615 MR). The electron beam is generated by a thermionically emitting, electrostatically focused, Pierce-type electron gun (250 kV, 250 A) from a SLAC klystron (Model 343). An emittance selector is used to limit the beam current to ~1 A. An assembly of focusing coils transports the electron beam into the rectangular stainless steel drift tube ($0.40'' \times 0.90''$), which also acts as the waveguide for the electromagnetic radiation. The beam is contained by a uniform 1.6 kG axial magnetic field produced by a solenoid.

A 65 period circularly polarized magnetic wiggler has a period $l_w = 3.5$ cm,

an amplitude B_w = 200-400 G, and is generated by bifilar conductors.[12,13] Since an aperture limits the size of the electron beam to $r_b \simeq 0.07 l_w$, the wiggler field appears nearly sinusoidal to the drifting electrons. At the wiggler entrance a slowly increasing field amplitude is produced by resistively loading the first six periods of the wiggler magnet.

The 2.7 m long drift tube acts as a rectangular waveguide whose fundmental TE_{10} mode has a cutoff frequency of 6.6 GHz. The drift tube closes upon itself and thereby forms a ring cavity 7.6 m in length (see Fig. 1a). The system is operated in a frequency range between 8 and 11 GHz. At those frequencies the empty waveguide can support only the fundamental (TE_{10}) mode, all higher modes being evanescent. The ring cavity loss is 5.5 dB. The single-pass FEL gain varies between 6 and 8.5 dB, so that the overall system gain is less than 3 dB. It is in this low net gain operating regime that all of our measurements are carried out, and where the periodic rf spikes are the clearest. In order to observe the rf spikes, the radiation field of the ring cavity is sampled by means of a 20 dB directional coupler and then measured with a calibrated crystal detector.

Figures 1b and 1c illustrate the time history of the beam energy and rf power as observed on an oscilloscope screen. Since our Marx accelerator has an RC droop with a 25 μs time constant, the electron beam energy sweeps through the range of values illustrated in Fig. 1b. Figure 1c shows that the overall rf pulse starts $\sim$7μs after the Marx ignition and lasts typically for 1 to 3 μs.

Expanding the oscilloscope time scale yields the observed micropulses shown in Fig. 2a. Placing a band pass filter (9.6-10.2 GHz) in the output arm of the directional coupler, reveals better the underlying micropulse structure, as illustrated in Fig. 2b. The filtered pulse is seen to be composed of a sequence of partially overlapping macropulses with random start-up times. Each macropulse consists of a series of micropulses within a bell-shaped macropulse envelope. The distance between two successive micropulses is 36 ns, which is the ring cavity round-trip time of a micropulse with a center frequency of f_0 =9.6 GHz. The micropulse width is 2-4 ns, and no significant broadening is observed over many round-trips. Filtering the feedback signal by

a high-pass filter (f >9.6 GHz.), installed in the return leg of the ring cavity (instead of filtering the sampled signal) leads to similar results.

As noted above, each of the overlapping macropulses starts at a random time. However, its appearance is correlated to spikes in the current density shown in Fig. 2c. The current density is measured by a tiny probe[13] partially inserted within the electron stream and placed ~1 m from the beginning of the bifilar helical wiggler (Fig. 1a).

The simplified linear model of the FEL oscillator in the time domain discussed below takes into account both the statistical features of the electron beam and the FEL interaction. Random fluctuations of the electron beam initiate the oscillation process. They are described by a shot-noise model[14-16] in which the density $n_i(t)$ is given by

$$n_i(t) = n_o + n_n \sum_i \delta(t - t_i), \tag{1a}$$

where t_i are random times distributed with a uniform density λ_e; consequently $\delta(t-t_i)$ are Poisson impulses. The correlation function of $n_i(t)$ is therefore given by

$$R_n(\tau) = n_n^2(\lambda_e^2 + \lambda_e \delta(\tau)). \tag{1b}$$

In what follows we apply the shot-noise model to the current spikes shown in Fig. 2c, i.e., to macroparticles rather than to single electrons. The average temporal density of the spikes is $\lambda_e \sim 5\mu s^{-1}$ as evaluated from experiments.

The FEL oscillator is modeled as a cascade of FEL blocks[17] as shown in Fig. 3. Each stage l in the cascade represents one round-trip time τ_d, where D is a delay element equivalent to the feedback waveguide section. Each FEL block ($FEL^{(l)}$) has two inputs, one for the EM wave E_i, and the other for the electron beam density fluctuations n_i. Due to the voltage droop in the electron beam, each FEL block has different parameters determined by their instantaneous values at $t = l\tau_d$. We assume that these parameters are almost stationary during one round-trip. The round-trip period is updated in each round-trip according to the instantaneous center frequency

of the rf. Linear transfer functions define the relation between the output $\tilde{E}_o(\omega)$ and the two independent inputs, $\tilde{E}_i(\omega)$ and $\tilde{n}_i(\omega)$. These are given, in the frequency domain, for each FEL block (l) by

$$\tilde{E}_o(\omega)|_{n_i=0} = T_E^{(l)}(\omega)\tilde{E}_i(\omega) \tag{2a}$$

$$\tilde{E}_o(\omega)|_{E_i=0} = T_n^{(l)}(\omega)\tilde{n}_i(\omega). \tag{2b}$$

The transfer functions $T_E(\omega)$ and $T_n(\omega)$ are found from the gain-dispersion equations for the pre-bunched FEL.[18]

The response in the time domain of the FEL oscillator to a single density impulse, given by $n(t) = n_0 + n_n\delta(t)$ for $n\tau_d < t < (n+1)\tau_d$, is found by an inverse Fourier transform on the cascade transfer function

$$h_{osc}(t, t_1 = 0) = \frac{1}{2\pi}\int_\omega T_n^{(0)}(\omega)\prod_{l=1}^{n} T_E^{(l)}(\omega)e^{i\omega t}d\omega. \tag{3}$$

The intensity of the impulse response $|h_{osc}(t, t_1 = 0)|^2$ is computed for the parameters of the FEL used in the experiment and is shown plotted as a function of time in Fig. 4a. Figure 4b shows the corresponding frequency sweep due to the change in accelerator voltage shown in Fig. 1b. The first micropulse is the instantaneous response of the FEL to the electron beam impulse, and is esentially the time-domain representation of the FEL spontaneous emission induced by the density fluctuations. The width of the first micropulse is comparable with the FEL slippage time,[19] $[(1/v_g) - (1/v_z)]\, L_W$, where v_g is the radiation group velocity, v_z is the axial electron beam velocity and L_w is the wiggler length. It is found both analytically and numerically that the tendency of the micropulse to broaden, due to the waveguide dispersion, is balanced by the FEL gain and phase shift. Consequently, the micropulse width is preserved in many round-trips. This confirms our experimental results, in which no significant micropulse broadening is observed.

The theoretically calculated impulse response intensity of the FEL oscillator shown in Fig. 4a is quite similar to the bell-shaped macropulses measured in the experiment, shown in Fig. 2b, as is the periodic micropulse structure.

In conclusion, we have reported what we believe are entirely new observations of an FEL operating near oscillation threshold. The observations show that the radiation field is composed of bursts with a periodic substructure correlated to bursts in the electron beam current. These studies may lead to a better understanding of the FEL oscillator start-up phase and to methods of generating very short, tunable micropulses in free electron lasers.

ACKNOWLEDGEMENTS

This work is supported in part by the National Science Foundation, the Air Force Office of Scientific Research and the Naval Research Laboratory. E. J. is supported by the Rothschild and Fulbright foundations.

References

1. P. W. Smith, *IEEE J. Quantum Electron.*, **3**, 627, (1967).

2. P. W. Smith, *Proc. IEEE*, **58**, 1342 (1970); for recent studies on ultrafast laser phenomena, see the special issue of *IEEE J. Quantum Electron.*, **25** (1989).

3. L. F. Mollenauer and R. H. Stollen, *Opt. Lett.*, **9**, 13 (1984)

4. N. M. Kroll and M. N. Rosenbluth, in *Physics and Quantum Electronics* (Addison-Wesley, Reading, MA, 1980), Vol. 7, p. 147.

5. R. W. Warren, B. E. Newnam, and J. C. Goldstein, *IEEE J. Quantum Electron.*, **21**, 882, (1985).

6. J. Masud, T. C. Marshall, S. P. Schlesinger, and F. G. Yee, *Phys. Rev. Lett.*, **56**, 1567 (1986).

7. W. B. Colson, *Nucl. Instrum. Methods Phys. Res.*, **A250**, 168 (1986).

8. J. C. Goldstein, B. W. Newnam, R. W. Warren, and R. L. Sheffield, *Nucl. Instrum. Methods Phys. Res.*, **A250**, 4 (1986).

9. B. A. Richman, J. M. J. Madey, and E. Szarmes, *Phys. Rev. Lett.*, **63**, 1682 (1989).

10. J. W. Dodd and T. C. Marshall, in FEL '89 Conference Digest, 11^{th} Int. Conf. on Free Electron Lasers, Naples, Florida, L. R. Elias and I. Kimel, Eds., IEEE-LEOS 1989.

11. E. Jerby, J. S. Wurtele and G. Bekefi, *Bull. Am. Phys. Soc.*, **35**, 1026 (1990).

12. J. Fajans, G. Bekefi, Y. Z. Yin, and B. Lax, *Phys. Fluids*, **28**, 1995 (1985).

13. K. Xu, G. Bekefi, and C. Leibovitch, *Phys. Fluids*, **B1**, 2066 (1989), and references therein.

14. H. A. Haus, *IEEE J. Quantum Electron.*, **17**, 1427 (1981).

15. P. Sprangle, C. M. Tang, and I. Bernstein, *Physical Review A*, **28**, 2300 (1983).

16. K. J. Kim, *Phys. Rev. Lett.*, **57**, 1871 (1986).

17. A. Gover, H. Freund, V. L. Granatstein, J. H. McAdoo, and C. M. Tang, *Infrared and Millimeter Waves*, vol. 11, ch. 8, K. J. Button, Ed., New York, Academic, 1984.

18. I. Schnitzer and A. Gover, *Nucl. Instrum. Methods Phys. Res.*, **A237**, 124 (1985). For a 2D derivation of Eqs. (4a,b), see E. Jerby, "Angular Steering of the FEL Far-Field Radiation Beam," to be published in *Phys. Rev. A*.

19. R. Bonifacio, C. Maroli and N. Piovella, *Optics Communications* **68**, 369 (1988).

Figure Captions

Figure 1 (a) Experimental arrangement showing the ring cavity of the FEL oscillator; (b) and (c) are typical oscilloscope traces of the beam voltage and a radiation burst, respectively.

Figure 2 Expanded oscilloscope traces of typical radiation bursts before (a), and after (b) filtering (see text); (c) typical bursts in the electron beam current density.

Figure 3 Schematic of the computational model of the FEL oscillator.

Figure 4 (a) The computed impulse response of the FEL oscillator (to be compared with the experimental result in Fig. 2b), and (b) the corresponding center frequency associated with each pulse.

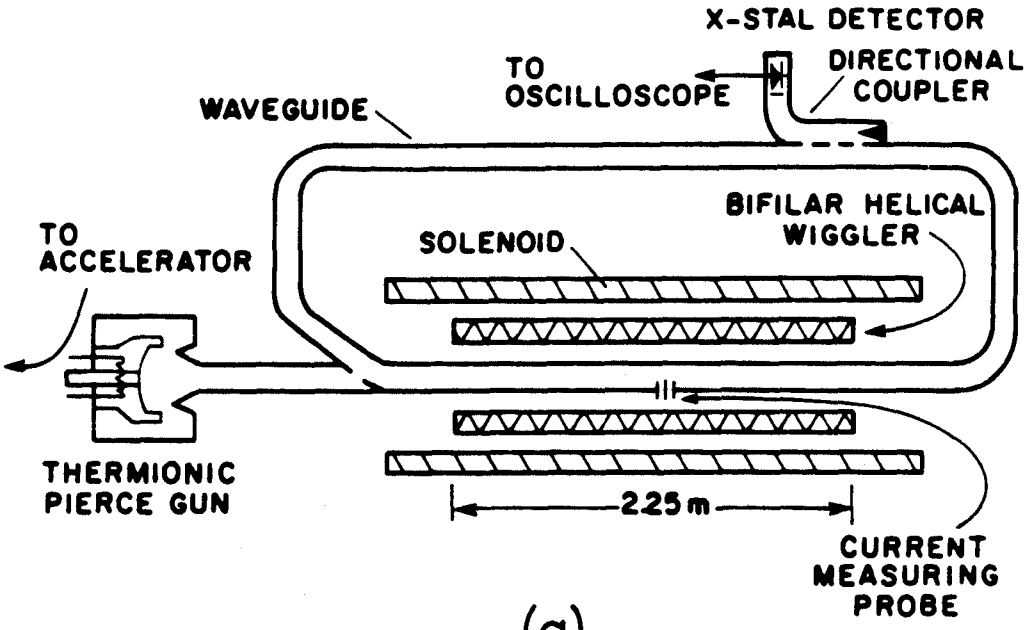

(a)

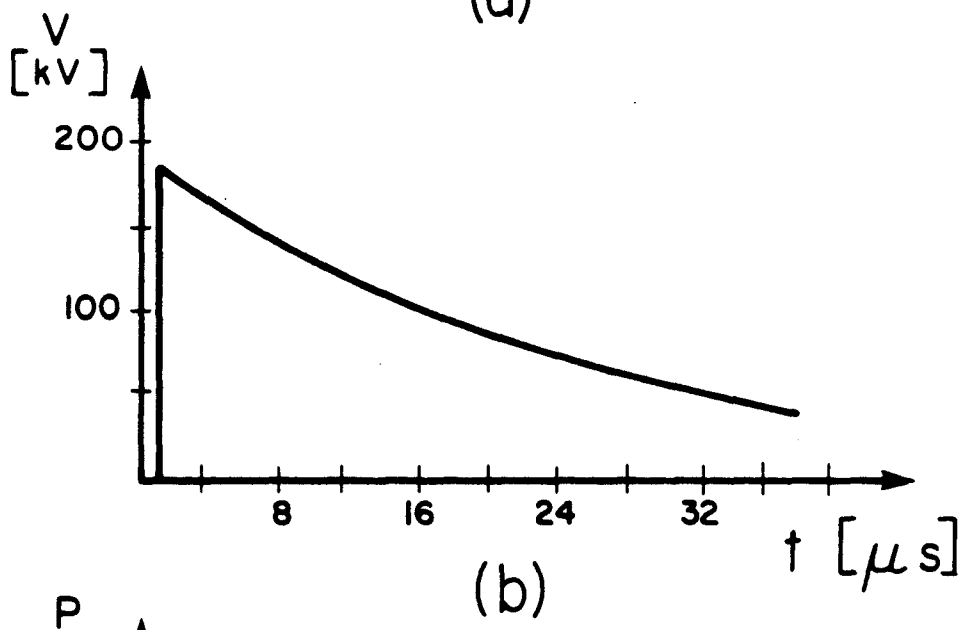

(b)

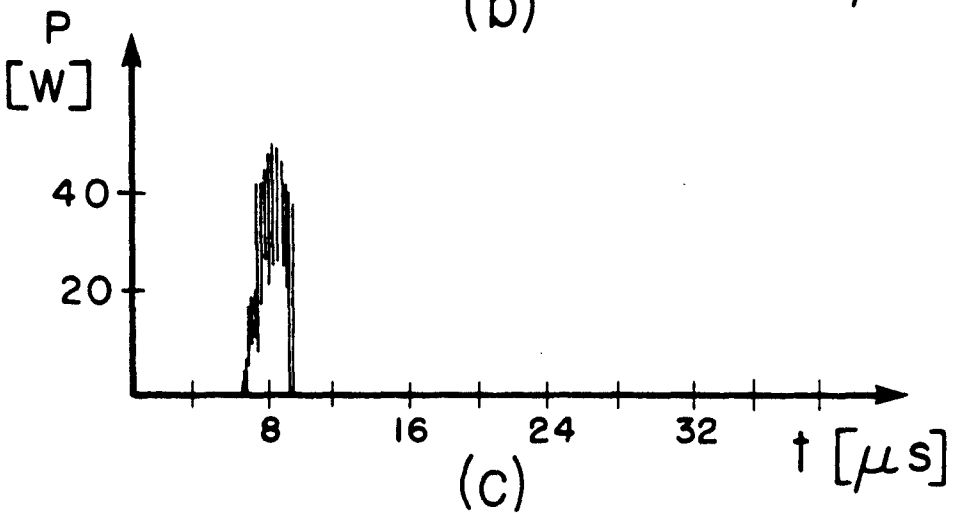

(c)

Fig.1 Jerby, Bekefi, Wurtele

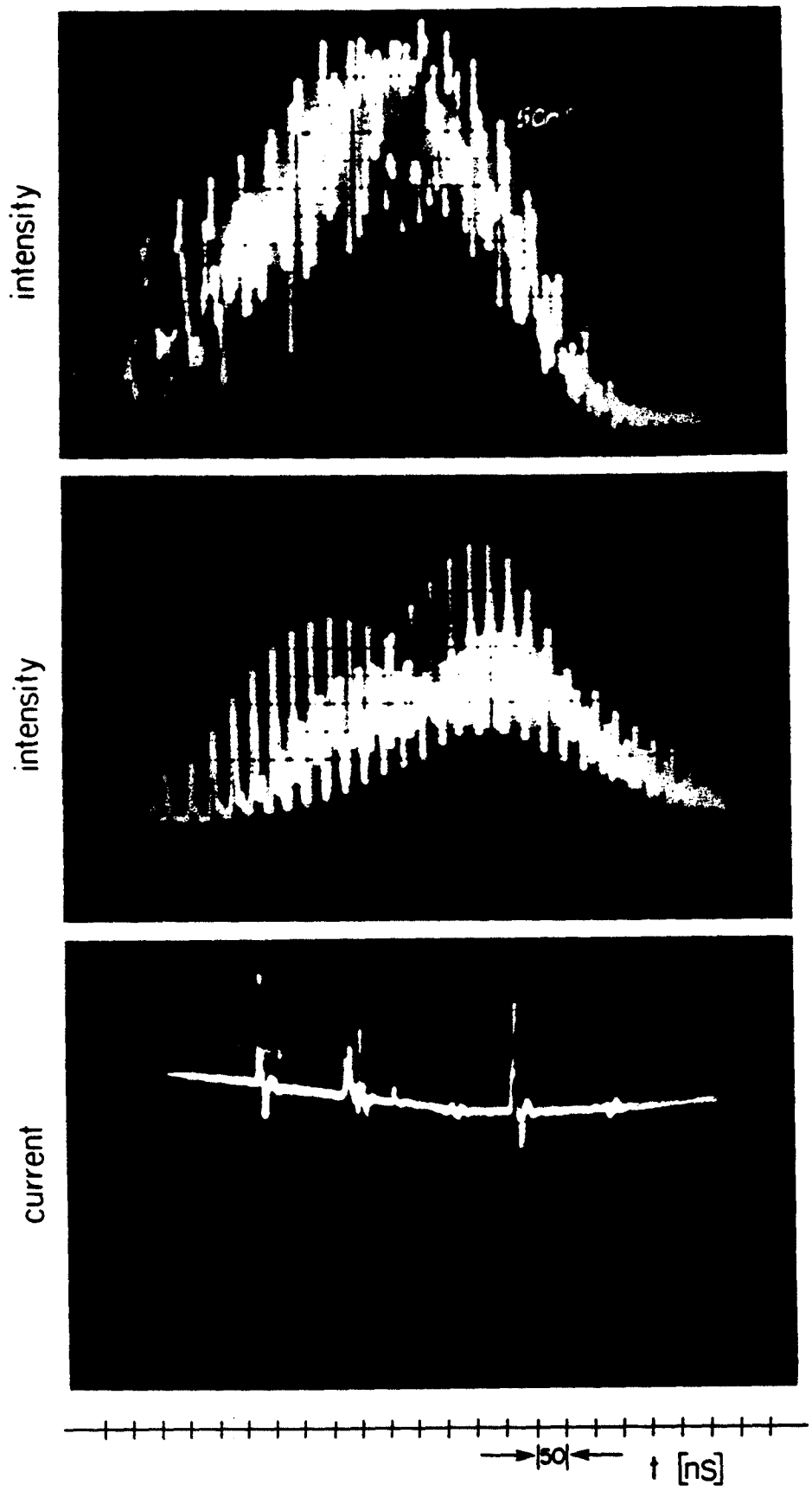

Fig.2 Jerby, Bekefi, Wurtele

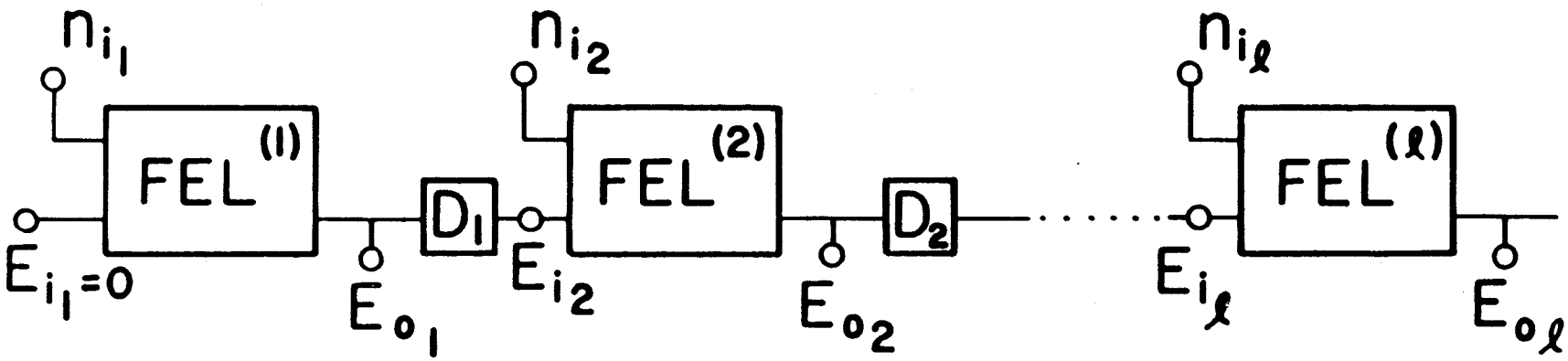

Fig.3 Jerby, Bekefi, Wurtele

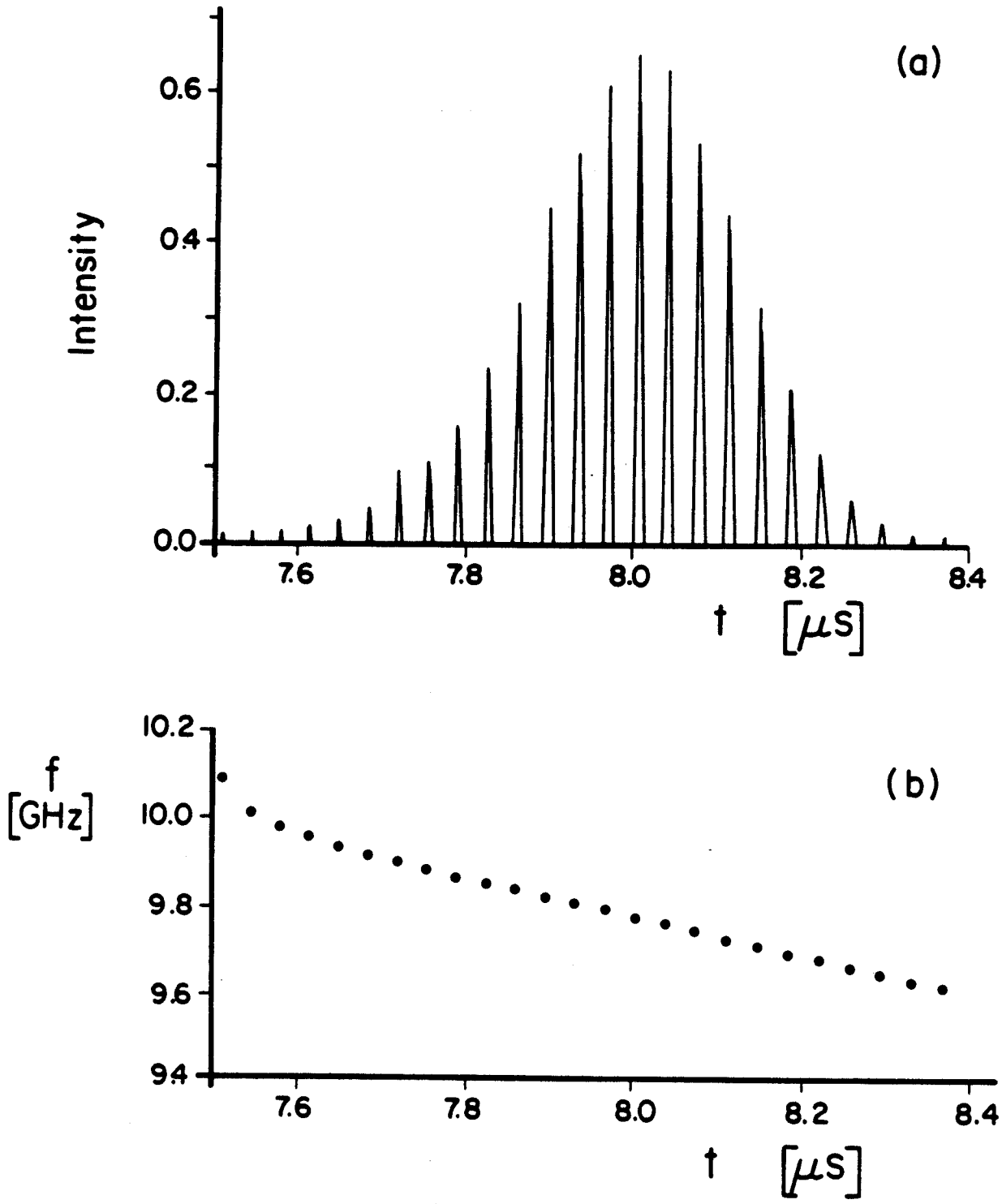

Fig.4 Jerby, Bekefi, Wurtele